

Fully Unsupervised Annotation of C. Elegans

Christoph Karg^{*,1,2}, Sebastian Stricker^{*,4}, Lisa Hutschenreiter⁴,
Bogdan Savchynskyy^{#,4}, and Dagmar Kainmueller^{#,1,2,3}

¹ Max-Delbrueck-Center for Molecular Medicine in the Helmholtz Association

² Helmholtz Imaging

³ University of Potsdam, Digital Engineering Faculty

⁴ Heidelberg University

^{*}, [#] equal contribution

✉ `{firstname.lastname}@mdc-berlin.de`,

✉ `{firstname.lastname}@iwr.uni-heidelberg.de`

Abstract. In this work we present a novel approach for unsupervised multi-graph matching, which applies to problems for which a Gaussian distribution of keypoint features can be assumed. We leverage cycle consistency as loss for self-supervised learning, and determine Gaussian parameters through Bayesian Optimization, yielding a highly efficient approach that scales to large datasets. Our fully unsupervised approach enables us to reach the accuracy of state-of-the-art supervised methodology for the use case of annotating cell nuclei in 3D microscopy images of the worm *C. elegans*. To this end, our approach yields the first unsupervised *atlas* of *C. elegans*, i.e. a model of the joint distribution of all of its cell nuclei, without the need for any ground truth cell annotation. This advancement enables highly efficient annotation of cell nuclei in large microscopy datasets of *C. elegans*. Beyond *C. elegans*, our approach offers fully unsupervised construction of cell-level atlases for any model organism with a stereotyped cell lineage, and thus bears the potential to catalyze respective comparative developmental studies in a range of further species.

Keywords: Multi-Graph Matching, Cycle-Consistency, Bayesian Optimization, Unsupervised Learning, *C. Elegans*, Cell-level Atlas

1 Introduction

The nematode worm *C. elegans* is a widely used model organism in biology, particularly valued for its cell-level stereotypicity: Its consistent body plan, composed from a fixed set of cells, allows to map cell-level observations across individuals into a common reference frame, enabling comprehensive studies of cellular processes, like e.g. gene expression [11,9].

A major bottleneck in such studies is the semantic annotation of individual cells with their unique biological names in 3D microscopy images, a task that is both time-consuming and requires rare expert knowledge. While state-of-the-art cell *instance* segmentation models achieve viably accurate results [15,19,4], the *semantic* annotation of these cells remains a key challenge.

The most successful strategy addressing this challenge is based on the construction of a statistical (Gaussian) atlas of cell nuclei from a given training set with ground truth annotations of semantic cell names [12,7,9]. Once such an atlas is built, new, unlabeled worms can be aligned using graph matching algorithms [3,5], allowing annotations to be transferred from the atlas to the target worm. However, a major drawback of such supervised approaches is their reliance on ground truth annotations, requiring manual expert labeling, which is an expensive, time-consuming, and error-prone process.

To overcome the reliance on ground truth annotations, we propose the first fully unsupervised approach for semantic cell annotation in *C. elegans*, eliminating the need for manual labeling. More specifically, we construct a statistical atlas of *C. elegans* from a training set containing only cell instance segmentations but no semantic annotations. Our approach advances upon recent work on deep unsupervised multi-graph matching [17]: Their method relies on a pre-trained feature extraction network, whose parameters it optimizes w.r.t. a self-supervised cycle-consistency loss. While their approach is viable for standard computer vision data, its reliance on a well-pre-trained backbone may hamper its generalization to intricate biomedical images, in particular to our use case of highly self-similar semantic classes. Thus instead of optimizing a feature extraction backbone, we leverage Bayesian Optimization to directly optimize Gaussian parameters of matching costs, which are assumed to govern keypoint features such as their centroids and pairwise offsets. Our unsupervised approach achieves **96.1%** accuracy, comparable to the 96.4% accuracy of a new state-of-the-art supervised baseline we also present here. In summary, we contribute:

- A novel Bayesian Optimization approach for learning Gaussian parameters of an unsupervised multi-graph matching objective;
- The first unsupervised statistical atlas of *C. elegans* established with our approach from a set of 3D microscopy images;
- A new *supervised* baseline for semantic annotation of *C. elegans* nuclei that beats the previous (supervised) state-of-the-art by a large margin;
- A comparative evaluation of our unsupervised approach against this supervised baseline, showing that unsupervised achieves comparable accuracy and thus effectively dissolving the long-standing bottleneck of obtaining ground truth annotations of *C. elegans* nuclei.

2 Background

To put our contribution into context, in the following, we first briefly review the mathematical description of a cell-level atlas of *C. elegans*, further referred as *atlas*, and formulate the problem of *worm-to-atlas* matching, both as given in [7]. Subsequently, we motivate and formulate the problem of *worm-to-worm matching* and *worm multi-matching* as performed in [16].

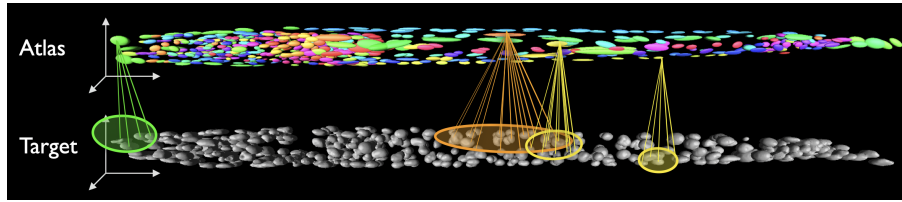


Fig. 1: Worm-to-atlas matching example. Atlas labels are illustrated by 3D ellipsoids representing the positional covariances Σ_i^{cen} . An optimal assignment between atlas labels and target segments is determined by solving a graph matching problem. To ensure computational efficiency, we sparsify the problem by restricting the set of possible assignments for each atlas label to a reduced subset of segments (colored ovals). The subset size depends on the covariances $\Sigma_i^{\{\text{cen}, \text{rad}\}}$ of the atlas label i .

2.1 Atlas-based annotation of C. elegans

Atlas as multivariate Gaussian. An atlas serves as a statistical model that captures the spatial distribution and structural variability of nuclei across multiple samples. Using the atlas representation suggested in [7] we model it as a multivariate Gaussian distribution. Let the finite set \mathcal{L} be the set of atlas nuclei, also called *labels*. Each nucleus $i \in \mathcal{L}$ is associated with two 3D Gaussian distributions $\mathcal{N}(\bar{x}_i^{\text{cen}}, \Sigma_i^{\text{cen}})$ for the position of its center x_i^{cen} and $\mathcal{N}(\bar{x}_i^{\text{rad}}, \Sigma_i^{\text{rad}})$ for its three principal axis radii x_i^{rad} . Here, $\bar{x}_i^{\text{cen}}, \bar{x}_i^{\text{rad}} \in \mathbb{R}^3$ are the mean position and radii vectors and Σ_i^{cen} and Σ_i^{rad} are the respective 3×3 covariance matrices. Furthermore, for any two nuclei $i, j \in \mathcal{L}$ it is assumed that the *offset vector* $x_{ij}^{\text{off}} = x_i^{\text{cen}} - x_j^{\text{cen}} \in \mathbb{R}^3$ is distributed as $\mathcal{N}(\bar{x}_{ij}^{\text{off}}, \Sigma_{ij}^{\text{off}})$. These distributions model correlated movement of different nuclei. In a supervised setting, all parameters of an atlas can be straightforwardly estimated from annotated samples as empirical means and covariances [7].

C. elegans annotation by worm-to-atlas matching. For a new target worm, we aim to label each of its nuclei with its unique biological name. Given an atlas (however obtained), as proposed in [7], this can be achieved by solving a *graph matching (GM)* problem [3] we term *worm-to-atlas matching*. This problem treats image segments (nuclei) as samples from the distribution defined by the atlas and consists in finding a correspondence between target segments and atlas labels that maximizes the probability defined by the atlas [8, Sec. 2].

The GM formalization considers two finite sets \mathcal{L} (here, *labels*) and \mathcal{S} (*segments*), whose elements must be matched to each other, as visualized in Figure 1. For each $i \in \mathcal{L}$ and $s \in \mathcal{S}$ the *unary* cost c_{is} of their matching is given, as well as the *pairwise* cost $c_{is, jt}$ for any pair $i, j \in \mathcal{L}$, $i \neq j$ if it is matched to any pair $s, t \in \mathcal{S}$, $s \neq t$. The goal of GM is to find a *matching* or *assignment* between elements of sets \mathcal{L} and \mathcal{S} that minimizes the total cost. This matching must satisfy the *uniqueness constraint*, that is, each element in \mathcal{L} must be assigned to *at most one* element in \mathcal{S} and vice versa. *At most one* implies that some elements may remain unassigned, which in our case may happen due to missing or superfluous

segments. In our application the unary costs are defined as

$$c_{is} = \lambda_{\text{cen}} d_{\text{cen}}(i, s) + \lambda_{\text{rad}} d_{\text{rad}}(i, s), \text{ where} \quad (1)$$

$$d_{\text{cen}}(i, s) = (\bar{x}_i^{\text{cen}} - x_s^{\text{cen}})^T (\Sigma_i^{\text{cen}})^{-1} (\bar{x}_i^{\text{cen}} - x_s^{\text{cen}}) \quad (2)$$

$$d_{\text{rad}}(i, s) = (\bar{x}_i^{\text{rad}} - x_s^{\text{rad}})^T (\Sigma_i^{\text{rad}})^{-1} (\bar{x}_i^{\text{rad}} - x_s^{\text{rad}}), \quad (3)$$

and the pairwise costs are defined as

$$c_{ij, st} = \lambda_{\text{off}} d_{\text{off}}(i, j, s, t) := \lambda_{\text{off}} (\bar{x}_{ij}^{\text{off}} - x_{st}^{\text{off}})^T (\Sigma_{ij}^{\text{off}})^{-1} (\bar{x}_{ij}^{\text{off}} - x_{st}^{\text{off}}), \quad (4)$$

where $\lambda_{\text{cen}}, \lambda_{\text{rad}}, \lambda_{\text{off}} > 0$ are weight parameters controlling the relevance of the respective features. With these costs, the GM objective can be phrased as follows:

$$\min_{x \in \{0,1\}^{|\mathcal{L}| \times |\mathcal{S}|}} \sum_{i,j \in \mathcal{L}} \sum_{s,t \in \mathcal{S}} C_{is,jt} \cdot x_{is} x_{jt} \quad (5)$$

$$\text{s.t.} \begin{cases} \forall i \in \mathcal{L} : \sum_{s \in \mathcal{S}} x_{is} \leq 1, \\ \forall s \in \mathcal{S} : \sum_{i \in \mathcal{L}} x_{is} \leq 1, \end{cases} \quad (6)$$

were the $x_{i,s}$ are binary variables that indicate whether atlas label i is assigned to target image segment s , and $C_{is,jt} = c_{is} + c_{jt} + c_{is,jt} - c_0$. Note, $c_0 > 0$ is a constant cost parameter, subtracted to allow for negative assignment costs, thus avoiding a trivial *nothing-assigned* solution.

One may *sparsify* the GM problem by forbidding any a-priori-known implausible matchings of segment s to label i by assigning the respective cost c_{is} an infinite value. This allows GM solvers that can leverage sparsity to deal with larger sets \mathcal{L} and \mathcal{S} . The GM problem is NP-hard, but for sparse problem instances with $|\mathcal{L}|, |\mathcal{S}| \approx 500 - 1000$ as in our case, there are methods able to find its accurate solutions in seconds, see the benchmark [3]. In our work, we employ the winner [5] of this benchmark and we apply the same sparsification for worm-to-atlas matching as described in [7].

2.2 C. elegans annotation by multi-graph matching

As a first step towards unsupervised annotation, we consider the case where per-nucleus resp. per-nucleus-pair covariance matrices $\Sigma_i^{\{\text{cen}, \text{rad}\}}$ resp. Σ_{ij}^{off} are unavailable, but instead, we assume that we can – somehow – at least obtain covariance matrices that are fixed across all nuclei resp. nuclei pairs, i.e., $\Sigma^{\{\text{cen}, \text{rad}, \text{off}\}}$. With this information, correspondences between target worms can still be determined [16]: For a pair of worms, we can establish a *worm-to-worm matching* problem, taking the same general form as the worm-to-atlas matching problems described in Sec. 2.1, albeit replacing any nucleus-specific covariance matrix with its cross-nuclei counterpart (i.e., we drop the indices i for all covariance matrices). Also, each nucleus-specific mean of the atlas (e.g. \bar{x}_i^{cen}) is replaced by the respective feature vector (x_i^{cen}) of the worm to be matched to the target worm.

Generalizing beyond pairs of worms, the problem considered in [16] is to achieve consistent pairwise matchings for a *set of worms*. This constitutes a

multi-graph matching (MGM) problem, which naturally extends the GM problem to a set of keypoint sets, $(\mathcal{S}^1, \dots, \mathcal{S}^N)$. The MGM objective is to find a *cycle consistent* correspondence between the keypoint sets, that minimizes the cost sum over all GM problems between the $\binom{N}{2}$ pairs of keypoint sets. Cycle consistency, as visualized in Figure 2, means transitivity of matchings, i.e., for any sequence of (keypoint) segments s_1, \dots, s_k over k different keypoint sets, s_i being matched to s_{i+1} for all $i < k$ implies that s_k is matched to s_1 . Cycle consistency across all triplets of keypoint sets is sufficient to ensure cycle consistency across all keypoint sets [16]. Cycle consistency of triplets can be straightforwardly captured as a set of linear constraints to be appended to a GM objective (see [16] for details), thus turning a GM into an MGM problem. Sparse MGM problems, i.e., MGMs with sparse GM subproblems as in our case, are solved in a highly efficient manner by the recently published algorithm of [6], which internally leverages [5] to solve GM subproblems.

A cycle consistent solution of an MGM problem naturally yields *cliques* of matched keypoints, comprising (at most) one segment per target worm. We assign a unique pseudo-label (in form of a "clique ID") to each clique and thus to each segment within the clique. In this scenario, unique pseudo-labels stand in place of unique biological ground truth names. Such MGM-based pseudo-label annotations may then serve as pseudo-ground truth to build an atlas used for worm-to-atlas matching, where we can leverage nucleus-specific covariances again instead of covariances that are fixed for all nuclei.

Parameters of the worm multi-matching problem are the covariance matrices $\Sigma^{\{\text{cen}, \text{rad}, \text{off}\}}$ and the cost weights $\lambda_{\text{cen}}, \lambda_{\text{rad}}, \lambda_{\text{off}}$. We further sparsify our *worm-to-worm matching* problems using three hyper-parameters $K_{\text{min}}, \tau_{\text{cen}}, \tau_{\text{rad}}$: We forbid all assignments where $d_{\text{cen}}(i, s)$ is above a certain threshold $\tau_{\text{cen}} > 0$, and proceed analogously with a threshold $\tau_{\text{rad}} > 0$. However, precomputing all possible unary costs c_{ij} , we allow at least the K_{min} lowest cost assignments of every nuclei. A further parameter is the subtracted cost constant c_0 which incentivizes non-trivial matchings. It effectively controls how many nuclei remain *unmatched*. We match as many nuclei as possible by setting c_0 to a large constant, exceeding any finite $c_{is} + c_{jt} + c_{is,jt}$.

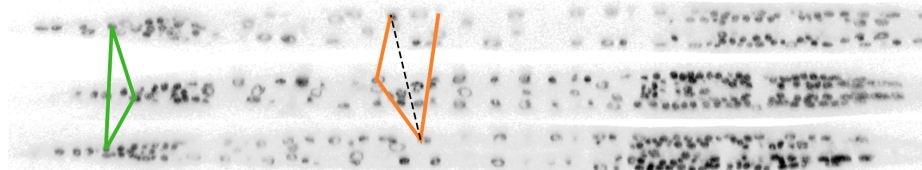


Fig. 2: Multi-graph matching example. Cell nuclei are matched across three exemplary worm instances. This results in either cycle consistent matchings (green) which form a clique, or inconsistent matchings (orange). Cycle consistency is necessary but not sufficient for correctness. Vice-versa, inconsistency entails error.

In [16] the covariance matrices are obtained from ground truth annotations via summary statistics over all nuclei in all annotated worms (instead of summary statistics per nucleus over all annotated worms). They furthermore use cost weights and sparsity hyper-parameters as determined via supervised validation in [7]. Their approach to worm-to-worm matching is thus supervised. In the next section, we propose a fully unsupervised approach.

3 Unsupervised Atlas Learning via Bayesian Optimization

We here propose an approach for fully unsupervised learning of all parameters of worm MGM. Note, when treating covariance matrices $\Sigma^{\{\text{cen,rad,off}\}}$ as learnable parameters their cost weight coefficients $\lambda_{\text{cen}}, \lambda_{\text{rad}}, \lambda_{\text{off}}$ become redundant and can be discarded. To further simplify the problem, we consider diagonal covariance matrices, since variance mainly differs in the three body axes, the latter being pre-determined by unsupervised rigid worm alignment. We thus only need to learn covariance matrices and sparsity hyper-parameters, $K_{\text{min}}, \tau_{\text{cen}}, \tau_{\text{rad}}$, yielding $3+3+3+3=12$ parameters in total. To this end we leverage MGM cycle consistency as self-supervised objective in a Bayesian Optimization framework, as described in the following.

Cycle consistency as described in section 2.2 has been shown to serve as self-supervisory objective in related works on deep MGM [17]. We employ the so called *synchronization* objective, see, e.g., [6, Sec. 7], as a loss. The synchronization objective counts the minimum number of adjustments needed to achieve cycle consistency, starting from an initially inconsistent solution. Its approximate computation is performed with the algorithm [6, Sec. 7]. While [17] have leveraged cycle consistency to fine-tune well-pre-trained parameters of a neural network via black-box differentiation, to our knowledge, we are first to employ cycle consistency as objective in a Bayesian Optimization approach.

Bayesian optimization (BO) [14] treats the objective as a random function over which it places a prior. A posterior is iteratively inferred by evaluating the objective within a sufficiently large search space. The obtained posterior then yields an acquisition function that determines the next query point. We use the Optuna framework [1] for BO, with default Tree-structured Parzen Estimator (TPE) [2] and multi-objective TPE [13] for optimization.

To achieve BO at viable computational efficiency, we select a subset of N_{cost} worms from the full set of atlas worms. For this subset, we solve all $\binom{N_{\text{cost}}}{2}$ worm-to-worm matching problems, then calculate the cycle consistency objective based on the returned solutions.

We learn parameters in a BO pipeline composed of three steps: 1) We first optimize the covariance parameters Σ_{cen} and Σ_{rad} necessary for unary costs in a 6-dimensional search space, discarding pairwise costs as well as sparsity hyper-parameters. Discarding pairwise terms here is vital as it turns the underlying matching problems into *linear assignment problems*, which are polynomial-time solvable. 2) We then optimize the three sparsity hyper-parameters in a 3-dimensional search space, still discarding pairwise terms. The goal of this step is

to make the matching problems as sparse and small as possible such that solving them with pairwise terms in the next step becomes feasible. This step involves multi-objective TPE [13], as we optimize for both sparsity and cycle consistency. 3) In this last step we include the pairwise costs of the GM problems and optimize the remaining three covariance parameters in Σ_{off} .

4 Results

Dataset. We showcase our approach on a dataset of 200 3D light microscopy images of *C. elegans* at the L1 larval stage [10]. In the following we refer to this dataset as **200worms**. Each worm at the L1 stage contains 558 nuclei, for which ground truth instance segmentations as well as full semantic annotations of nuclei are available as described in [9]. The dataset provides three sets of 100 worms: A training set, and two test sets. We use the same test set as [9] to allow for comparable results. In an unsupervised pre-processing step, we rigidly align the body axes and barycenters of all worms as in [7].

Supervised baseline. We achieve a supervised baseline using standard atlas construction from the training set (Sec. 2.1) and worm-to-atlas matching of the test set via the state-of-the-art GM solver from [5]. Additionally, we apply BO to improve cost weights $\lambda_{\text{cen}}, \lambda_{\text{rad}}, \lambda_{\text{off}}$ where the objective is to maximize matching accuracy on the dataset from [7], while retaining the same sparsity hyper-parameters.

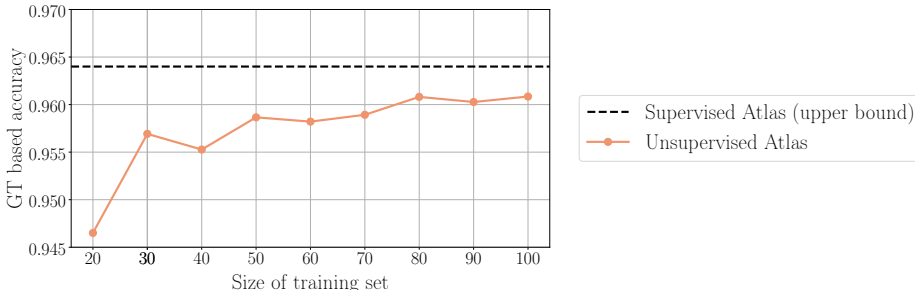
Unsupervised atlas-to-worm matching. We employ our BO approach with cycle consistency objective to learn the parameters of worm MGM from a subset of $N_{\text{cost}} = 15$ worms from the training set as described in Sec. 3. We then leverage the MGM solution obtained on the whole training set with optimal parameters as pseudo ground-truth to build an unsupervised atlas as described in Sec. 2.2, and perform worm-to-atlas matching of the test worms as described in Sec. 2.1.

Evaluation metrics. In a supervised scenario, accuracy can be defined as the proportion of correctly assigned ground truth labels among all 558 target nuclei. As a comparable metric in an unsupervised scenario, we define **Ground truth (GT) based accuracy**. For this metric, we use ground truth labels of the training worms to induce a semantic labeling of the unsupervised atlas by means of greedy max-voting. Note, this metric requires ground truth semantic labels for both training- and test worms, whereas in real-world unsupervised scenarios, ground truth may not be available for training worms.

To also evaluate *without any semantic nucleus labels*, we use the Rand Index, which relies solely on ground truth pairwise correspondences. All evaluated methods—supervised atlas, unsupervised atlas, and multi-worm matching—induce a clique decomposition on test nuclei, forming clusters that can be compared to the ground truth clustering. The **Adjusted Rand Index (ARI)** [18] quantifies the similarity between predicted and ground truth clusterings.

Table 1: Comparative evaluation of supervised- vs. unsupervised atlas-based *C. elegans* annotation on our 100/100 train/test split of `200worms`.

Method	GT based accuracy	ARI
Supervised Atlas	0.964 ± 0.019	0.941
Unsupervised Atlas	0.961 ± 0.020	0.933

**Fig. 3:** Impact of training set size on unsupervised atlas accuracy. As upper bound we here show the best supervised baseline, obtained with a supervised atlas built from all 100 training worms.

Supervised baseline. Our supervised baseline defines the new state-of-the-art on `worms200`, achieving 0.964 ± 0.02 accuracy, outperforming the recent results of [9], 0.93 ± 0.11 , as well as our re-implementation of [7], 0.91 ± 0.05 .

Unsupervised vs supervised. Table 1 lists supervised and unsupervised results of atlas-based *C. elegans* annotation in terms of error metrics. Our unsupervised atlas achieves a GT-based accuracy of 0.961, closely matching the 0.964 achieved with our SOTA supervised baseline, demonstrating the competitiveness of our unsupervised approach.

Training set size. To assess the impact of atlas size, i.e., the number of worms from which an atlas is built, we build atlases from selections of $N \in \{20, 30, \dots, 100\}$ of the 100 training worms in the `200worms` dataset. Figure 3 shows the impact of training set size on unsupervised atlas accuracy on the test worms, compared to the achieved accuracy of our supervised atlas baseline, serving as an upper bound. We observe a gradual improvement that stabilizes beyond a few dozen training worms. These results suggest that a well-performing unsupervised atlas can be constructed from such number of training worms.

5 Discussion

We introduced the first unsupervised cell-level atlas for *C. elegans*, alleviating the need for manual annotations while achieving accuracy comparable to state-of-the-art supervised methods, thus effectively eliminating a long-standing

bottleneck in *C. elegans* research. Our approach leverages multi-graph matching and Bayesian Optimization with cycle-consistency objective, enabling fully automated atlas construction.

While effective, we currently only applied our method to the L1 stage of *C. elegans*, the most popular cell-level stereotypical model organism. Extending it to other stereotypical organisms or organs such as ascidians or drosophila larval brains would serve to validate its broader applicability. Additionally, our use of radii as nuclei shape descriptors could be improved to adopt finer, possible learned geometric features to further enhance matching accuracy.

Acknowledgments. This work was supported by the German Research Foundation projects 498181230 and 539435352. Authors further acknowledge facilities for high throughput calculations bwHPC of the state of Baden-Württemberg (DFG grant INST 35/1597-1 FUGG) as well as Center for Information Services and High Performance Computing (ZIH) at TU Dresden.

References

1. Akiba, T., Sano, S., Yanase, T., Ohta, T., Koyama, M.: Optuna: A next-generation hyperparameter optimization framework. In: Proceedings of the 25th ACM SIGKDD International Conference on Knowledge Discovery and Data Mining (2019)
2. Bergstra, J., Bardenet, R., Bengio, Y., Kégl, B.: Algorithms for hyper-parameter optimization. *Advances in neural information processing systems* **24** (2011)
3. Haller, S., Feineis, L., Hutschenreiter, L., Bernard, F., Rother, C., Kainmüller, D., Swoboda, P., Savchynskyy, B.: A comparative study of graph matching algorithms in computer vision. In: European Conference on Computer Vision. pp. 636–653. Springer (2022)
4. Hirsch, P., Kainmueller, D.: An auxiliary task for learning nuclei segmentation in 3d microscopy images. In: Medical Imaging with Deep Learning. pp. 304–321. PMLR (2020)
5. Hutschenreiter, L., Haller, S., Feineis, L., Rother, C., Kainmüller, D., Savchynskyy, B.: Fusion moves for graph matching. *IEEE International Conference on Computer Vision* (accepted as **oral**, 2021), <https://arxiv.org/pdf/2101.12085.pdf>
6. Kahl, M., Stricker, S., Hutschenreiter, L., Bernard, F., Savchynskyy, B.: Unlocking the potential of operations research for multi-graph matching (06 2024). <https://doi.org/10.48550/arXiv.2406.18215>
7. Kainmueller, D., Jug, F., Rother, C., Myers, G.: Active Graph Matching for Automatic Joint Segmentation and Annotation of *C. elegans*. In: Golland, P., Hata, N., Barillot, C., Hornegger, J., Howe, R. (eds.) *Medical Image Computing and Computer-Assisted Intervention – MICCAI 2014*, vol. 8673, pp. 81–88. Springer International Publishing, Cham (2014). https://doi.org/10.1007/978-3-319-10404-1_11, series Title: Lecture Notes in Computer Science
8. Lempitsky, V., Rother, C., Roth, S., Blake, A.: Fusion moves for markov random field optimization. *IEEE Transactions on Pattern Analysis and Machine Intelligence* **32**(8), 1392–1405 (2010). <https://doi.org/10.1109/TPAMI.2009.143>
9. Li, Y., Chen, S., Liu, W., Zhao, D., Gao, Y., Hu, S., Liu, H., Li, Y., Qu, L., Liu, X.: A full-body transcription factor expression atlas with completely resolved cell

- identities in *C. elegans*. *Nat Commun* **15**(1), 358 (Jan 2024). <https://doi.org/10.1038/s41467-023-42677-6>, <https://www.nature.com/articles/s41467-023-42677-6>
10. Li, Y., Liu, X.: Image stacks for full-body transcription factor expression atlas with completely resolved cell identities in *C. elegans* (Oct 2023). <https://doi.org/10.5281/zenodo.7628038>, <https://doi.org/10.5281/zenodo.7628038>
 11. Liu, X., Long, F., Peng, H., Aerni, S.J., Jiang, M., Sánchez-Blanco, A., Murray, J.I., Preston, E., Mericle, B., Batzoglou, S., Myers, E.W., Kim, S.K.: Analysis of cell fate from single-cell gene expression profiles in *C. elegans*. *Cell* **139**(3), 623–633 (October 2009). <https://doi.org/10.1016/j.cell.2009.08.044>
 12. Long, F., Peng, H., Liu, X., Kim, S.K., Myers, E.: A 3D digital atlas of *C. elegans* and its application to single-cell analyses. *Nat Methods* **6**(9), 667–672 (Sep 2009). <https://doi.org/10.1038/nmeth.1366>, <https://www.nature.com/articles/nmeth.1366>
 13. Ozaki, Y., Tanigaki, Y., Watanabe, S., Onishi, M.: Multiobjective tree-structured parzen estimator for computationally expensive optimization problems. In: Proceedings of the 2020 Genetic and Evolutionary Computation Conference. p. 533–541. GECCO '20, Association for Computing Machinery, New York, NY, USA (2020). <https://doi.org/10.1145/3377930.3389817>, <https://doi.org/10.1145/3377930.3389817>
 14. Snoek, J., Larochelle, H., Adams, R.P.: Practical bayesian optimization of machine learning algorithms (2012), <https://arxiv.org/abs/1206.2944>
 15. Stringer, C., Wang, T., Michaelos, M., Pachitariu, M.: Cellpose: a generalist algorithm for cellular segmentation. *Nature Methods* **18**, 1–7 (01 2021). <https://doi.org/10.1038/s41592-020-01018-x>
 16. Swoboda, P., Kainmüller, D., Mokarian, A., Theobalt, C., Bernard, F.: A convex relaxation for multi-graph matching. In: Proceedings of the IEEE Conference on Computer Vision and Pattern Recognition. pp. 11156–11165 (2019)
 17. Tourani, S., Khan, M.H., Rother, C., Savchynskyy, B.: Discrete cycle-consistency based unsupervised deep graph matching. In: Proceedings of the AAAI Conference on Artificial Intelligence. vol. 38, pp. 5252–5260 (2024)
 18. Vinh, N.X., Epps, J., Bailey, J.: Information theoretic measures for clusterings comparison: Variants, properties, normalization and correction for chance. *Journal of Machine Learning Research* **11**(95), 2837–2854 (2010), <http://jmlr.org/papers/v11/vinh10a.html>
 19. Weigert, M., Schmidt, U.: Nuclei instance segmentation and classification in histopathology images with stardist. In: The IEEE International Symposium on Biomedical Imaging Challenges (ISBIC) (2022). <https://doi.org/10.1109/ISBIC56247.2022.9854534>